

Ion beam synthesis of AlN nanostructured thin films

E. VALCHEVA, D. MANOVA, S. MÄNDL, S. ALEXANDROVA, J. LUTZ, S. DIMITROV

^a Faculty of Physics, Sofia University, 5 J. Bourchier Blvd, 1164 Sofia, Bulgaria,

^b Institute for Surface Modification, Permoserstr. 15, 04318 Leipzig, Germany

^c Department of Applied Physics, Technical University, 8 Kl. Ohridski Blvd., 1797 Sofia, Bulgaria

The possibility of thin AlN film formation in SiO₂/Si by sequential implantation of Al and N using a plasma ion immersion implantation is reported. The ion profiles in the silicon dioxide substrate are evaluated through Monte Carlo simulations. The chemical composition and the nature of the chemical bonds are determined by Raman spectroscopy. The formation of randomly oriented nanoclusters of h-AlN is detected, without thermal annealing. The formation energies of Al-N, Al-O, Si-O and Si-N bonds are taken into consideration, in discussing the nanoclustering of the implanted species to form nanostructured AlN films.

(Received November 1, 2006; accepted December 21, 2006)

Keywords: AlN, Ion beam synthesis, Ion profiles, Nanoclustering

1. Introduction

AlN is a III-V compound that has attracted interest for its possible applications in optoelectronics, high-temperature electronics and as anti-wear coatings [1]. Along with many interesting properties such as a large bandgap (6.2 eV), high thermal conductivity, high acoustic velocity, high stability at high temperature, high hardness and enhanced corrosion resistance, AlN has the potential to be integrated with well-developed silicon microelectronic circuits. Because of the lack of large scale bulk samples and a suitable substrate for epitaxial growth, AlN thin films grow heteroepitaxially on various substrates. Silicon is of special interest, because of its importance in contemporary device technology and the possibility to integrate different functions, e.g., UV-detection or emission and Si-ICs on a common substrate. An important point is that AlN has a coefficient of thermal expansion similar to that of silicon.

In recent years, a trend of significant importance has been the synthesis of AlN nanostructured thin films. The formation of such films by a variety of deposition methods has frequently been reported, such as the use of chemical deposition methods [2], dc magnetron sputtering [3], etc. Ion implantation is used as a versatile tool for the formation of compound semiconductor nanocrystal precipitates in a host medium, with the aim of forming quantum dots for use in device technology. Numerous studies describe the formation of AlN nanostructure layers by the N⁺ ion nitriding of aluminium [4]. The most important advantage of using implantation is the ability to obtain the best control and precision over the formation of the films in the substrates, in all three dimensions. This method has been applied mostly for the formation of Si and Ge nanoparticles in a SiO matrix.

In this study, the possibility of thin nanostructured AlN film formation in amorphous thermal SiO₂ on Si substrates, by sequential implantation of aluminum and nitrogen ions, is discussed. As an implantation technique,

plasma ion immersion implantation (PIII) is considered [5]. Beside the ability to implant large areas simultaneously, it is a very attractive method for obtaining broad profiles within one implantation, due to the energy spread and the presence of multiple ions in the plasma. Furthermore, careful adjustment of the parameters will allow the parallel implantation of Al and N in further experiments. The aim of the present work is to identify the formation and crystallization of AlN, after sequential implantation at room temperature.

2. Experimental details

Aluminium and nitrogen have been implanted into layers of amorphous thermal silica (SiO₂), in an attempt to bond Al with N and form the binary compound AlN. PIII was performed in a UHV system equipped with a 40.68 MHz RF plasma source and a cathodic arc, to produce the Al ions. In this set of experiments, sequential implantation of Al and N was performed without breaking the vacuum between the implantations. The substrate materials were blank Si(100) samples, together with SiO₂/Si samples of different oxide thickness. The acceleration voltage was either 5 or 10 kV, hence kinetic energies between 2.5 and 10 keV were obtained for N⁺ and N₂⁺ ions, while 5 to 30 keV were obtained for Al⁺, Al²⁺ and Al³⁺ ions. The high voltage pulses had a repetition rate of 3 kHz at a pulse length of 15 μs. Allowing for the different ion masses, a considerable overlap of the implanted profiles could be expected in this way, with the implanted atoms distributed from the surface down to about 50 nm, assuming that surface sputtering is negligible. The incident ion fluencies were varied from 8×10¹⁶ to 5×10¹⁷ Al and N atoms/cm². The resulting concentration should be around 10 – 25 at.%, still favoring the formation of stoichiometric AlN nanocrystals while avoiding the formation of a closed buried AlN layer. We should note that although the temperature is not intentionally increased, the ion collisions raise the local temperature of the matrix, but it

does not exceed 100°C. The experimental details and sample notations are given in Table 1.

Experiments on reversing the order of implantation, i.e. N before Al, and joint Al+N implantation are in progress.

Table 1. The regimes of PIII for aluminum and nitrogen into SiO₂.

Regime	Aluminum		Nitrogen	
	Voltage (kV)	Fluence (cm ⁻²)	Voltage (kV)	Fluence (cm ⁻²)
#1	7.5	8×10 ¹⁶	5	1×10 ¹⁷
#2	10	4×10 ¹⁷	5	5×10 ¹⁷
#3	10	8×10 ¹⁶	10	1×10 ¹⁷
#4	10	4×10 ¹⁷	10	5×10 ¹⁷

The chemical composition and the nature of the chemical bonds were determined by micro-Raman spectroscopy. As the positions of the TO and LO phonon bands depend on the crystallographic orientation of the facets, Raman scattering at normal incidence can provide a means to detect the presence and orientation of any AlN crystallite. Such a local nondestructive technique is very useful for evaluating samples of nanostructured AlN. The Raman spectra were measured using a Microdil 28 Dilor triple spectrometer and the 488 nm line of an Ar⁺ laser. The diameter of the laser spot was 1–2 μm, and the spectral resolution was about 1 cm⁻¹. The experiment was conducted in a backscattering geometry.

3. Modeling of AlN synthesis

The ion profiles in the silicon substrate were evaluated through Monte Carlo simulations. In PIII, the incident ions have a distribution of energies. A fraction of the ions (typically 5–10%) are implanted at energies that are less than the magnitude of the applied voltage, due to a finite pulse rise time and collisions within the plasma sheath at sufficiently high gas pressures. For the present conditions, the lower value 5% is applicable.

Literature data are available to estimate the ion species distribution for nitrogen plasmas from N₂ gas and aluminium plasmas from a cathodic arc. The nitrogen plasma will consist of 90% N₂⁺ and 10% N⁺ [6], whereas 38% Al⁺, 51% Al²⁺, and 11% Al³⁺ are appropriate for Al [7]. This mixture of different ion species without mass separation leads to a broader distribution of the implanted atoms, compared with conventional ion beam methods. The corresponding depth distributions could be calculated using the transport of ions in a matter simulation (SRIM version 2003) [8]. In Fig. 1, these simulated distributions of Al and N ion species for regime 2 are presented.

The projected range, using the nominal energy, is about 50% higher for N than for Al. However, the actual charge state distributions, multiply charged Al and molecular N₂ ions, reverse the situation: a wider distribution is obtained for Al than for N. Collisions within the plasma sheath broaden both distributions towards the surface, hence box-like profiles with a short tail can be

expected from both elements. However, the charge distribution of Al is valid at the cathode only [7]. Collisions within the expanding plasma will lead to a lower average charge state.

Furthermore, subsequent surface erosion by sputtering is not included in these calculations, as well as nitrogen desorption. Hence, different profiles could be expected when changing the order of the implantations. For the present ion fluence, a total sputter rate of less than 5–10 nm is expected from SRIM calculations, and was confirmed by spectroscopic ellipsometry. Implantation in the sequence Al-N should lead to a slightly better overlap of the distributions than for N-Al. Simultaneous implantation will remedy this problem, albeit that additional experiment is necessary to optimize the process parameters for the implantation of N/Al at a ratio of 1:1.

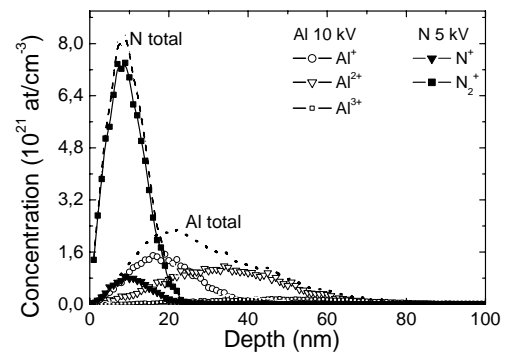


Fig. 1. Simulated depth distributions of Al and N ions in sample 2.

Secondary ion mass spectrometry (SIMS) depth profiling confirmed the presence of Al and N up to a depth of 80 nm, with AlN cluster ions detected in the range 20–40 nm, in conjunction with atomic Al and N ions.

4. Results and discussion

Fig. 2 shows representative Raman spectra of samples from different implantation regimes. The spectra reveal, in addition to the main O(Γ) peak of the Si substrate at 520 cm⁻¹, a band of spectral features between 600 and 700 cm⁻¹ where the optical phonon modes of AlN are expected to appear. The modes present in Fig. 2(b) at 612, 654, 671 cm⁻¹ can be indexed to the A₁(TO), E₂(high), and E₁(TO) phonon frequencies of a wurtzite-structured AlN (h-AlN) crystal, respectively [9]. This is evidence for the existence of randomly oriented AlN crystallites, with a size and shape distribution. It is known that microcrystals smaller than 30 nm lead to a downshift and broadening of the modes [10]. The E₂(high) phonon frequency at 654 cm⁻¹ shows a low-energy shift compared to the theoretical value of 657.4 cm⁻¹ [9], which appears as a result of the nanosize effect. According to [11] the mode at 816 cm⁻¹ can be attributed to amorphous material. A dependence on the

technological regime is clearly seen. Sample 4 reveals the $A_1(\text{TO})$, E_2 and $E_1(\text{TO})$ modes; sample 3 also shows two broader bands corresponding to A_1 and E_1 symmetry, sample 2 shows a broad structureless band of amorphous-like nature. Similar Raman spectra have been reported [12] for nanocrystalline AlN deposited by laser-assisted deposition. The spectra in the $600 - 700 \text{ cm}^{-1}$ region represent very well the calculated and reported [13] phonon density of states of AlN and the Raman spectra measured on Er-implanted AlN. Heavily disordered systems such as ion-implanted or low-temperature grown crystals are known to

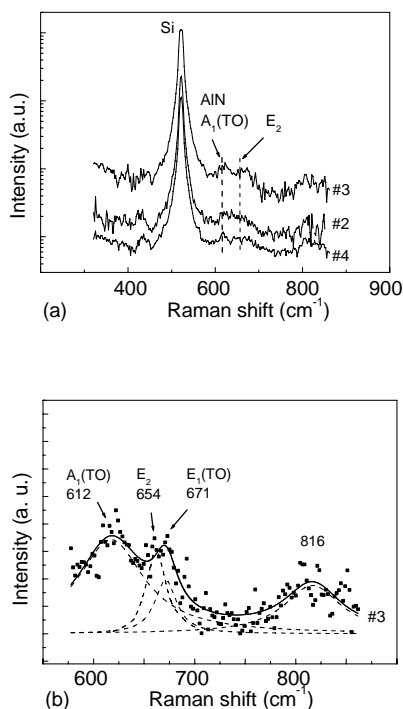


Fig. 2. (a) Micro-Raman spectra of samples 2, 3 and 4; the spectra are presented in logarithmic form and are shifted along the y axis. (b) Lorentzian deconvoluted spectrum of sample 4.

exhibit disorder-activated Raman scattering (DARS) modes. DARS occurs as a result of phonon confinement to nanosized defect-free regions. This confinement relaxes the Raman selection rules, allowing phonons with wavevectors $q \neq 0$ to contribute to the first-order Raman scattering. Consequently, DARS reflects the phonon density of states of the lattice, and usually exhibits broad spectral features. Thus we can conclude that in all three samples, amorphous as well as nanocrystalline AlN is formed.

Sequential high dose ion implantation is being used for the formation of compound nanoclusters in an oxide matrix. In general, the formation process depends on the existence of stable compounds of the two implanted species - Al and N in the case of AlN. To a first approximation, phase diagrams can be used to predict the product. According to the Al-N phase diagram, there is no stable phase of AlN_x ($x \neq 1$) [14]. During the implantation

process, both the implanted ions and the silicon compete for the oxygen in the oxide substrate. The formation of nitrides and oxynitrides such as SiN_x and SiO_xN_y , or AlON could not be excluded. According to the Gibbs free energies of formation (Table 2) the lower probability reaction to occur is between Al and N [15]. A decomposition reaction of SiO_2 to form SiO and $(1/2) \text{O}_2$ (g) reacting with Al may take place during the interaction with the high energy ions, but this reaction requires a temperature of $> 900^\circ$ [16]. A contribution of O from the SiO_2 substrate to react with the high energy Al particles could not be thus eliminated. Furthermore, for a more detailed description of the detected nanoclusters, additional investigations of the short-range order are necessary, by means of electron diffraction and imaging.

Table 2. Gibbs free energies of formation of stable compounds of Al, N, Si and O ions.

	AlN	AlO_x	Si_xN_y	SiO_2
ΔG_f (kJ/mol)	-318.1	-1582.3	-744.75	-857.7

5. Conclusions

We have presented the first indications of the formation of AlN nanoclusters in a silicon dioxide matrix, by means of ion-beam assisted synthesis using PIII. Raman scattering experiments showed the existence of randomly oriented AlN crystallites, with a size and shape distribution on the nanometer scale. At higher fluences and energies, amorphous material was also present. The synthesis of the nanoclusters was observed without annealing.

Acknowledgements

This study was supported by Grant No. D01-79 from DAAD and the Ministry of Education and Science of Bulgaria.

References

- [1] M. E. Levinstein, S. L. Rumyantsev, M. S. Shur, Properties of Advanced Semiconductors Materials, John Wiley & Sons, New York, (2001).
- [2] K. Sardar, C.N.R. Rao, Solid State Sciences **7**, 217 (2005).
- [3] F. Engelmark, G. F. Iriarte, I.V. Katardjiev, A. Harsta, U. Smith, S. Berg, J. Vac. Sci. & Technol. A **18**, 1609 (2002).
- [4] D. Manova, P. Huber, S. Sienz, J. W. Gerlach, S. Mändl, B. Rauschenbach, J. Vac. Sci. Technol. A **20**, 206 (2002).
- [5] A. Anders, Handbook of Plasma Immersion Ion Implantation & Deposition, Wiley Interscience, (2000).
- [6] K. S. Fancey, Vacuum **46**, 695 (1995).

- [7] A. Anders, Phys. Rev. E **55**, 969 (1997).
- [8] J. F. Ziegler, J. B. Biersack, U. Littmark, The Stopping and Range of Ions in Matter, Pergamon, Oxford (1985).
- [9] T. Prokofyeva, et al., Phys. Rev. B, **63**, 125313 (2001).
- [10] H. Richter, Z.P. Wang, L. Ley, Solid State Commun. **39**, 625 (1981).
- [11] C. Carlone, K. M. Lakin, H. R. Shanks, J. Appl. Phys. **55**, 4010 (1984).
- [12] Y. Lu, Z. Ren, T. Chong, B. Cheong, S. Chow, J. Wang, J. Appl. Phys. **87**, 1540 (2000).
- [13] V. Yu. Davydov, et al., Phys. Rev. B **58**, 12 899 (1998).
- [14] T. Reier, J.W. Schultze, W. Österle, Chr. Buchal, Surf. and Coat. Technol. **103**, 415 (1998).
- [15] CRC Handbook of Chemistry and Physics, ed. D. R. Lide, CRC Press, Boca Raton, FL (1992).
- [16] A. J. Moulson, J. Mat. Sci. **14**, 1017 (1979).

*Corresponding author: epv@phys.uni-sofia.bg